Model simulations of tsunami generated by the Storegga slide

C.B. Harbitz

Department of Mathematics, Mechanics Division,

University of Oslo,

P.O.Box 1053 Blindern, 0316 OSLO 3, Norway

June 25, 1991

Abstract

A mathematical model based on the hydrodynamic shallow water equations is developed for numerical simulation of water waves generated by the submarine Storegga Slides on the Norwegian continental slope. The equations are solved numerically by a finite difference technique. Computations of wave amplification effects reveal run-up heights between 5 and 8 m in exposed areas along the eastern coast of Greenland, Iceland and Scotland and the western coast of Norway. The calculated run-up heights agree remarkably well with possible tsunami wave heights deduced from geological evidences along the eastern coast of Scotland. The generated wave heights are strongly dependent on the acceleration of the slide. The effects of shear stress at the interface between the water and the slide body, has turned out to be important.

1

1 Introduction

1.1 Introductory remarks

This paper is motivated by the reports by Dawson et al. (1988) and Long et al. (1989), where the occurrence of sand layers interbedded in terrestrial peat along the eastern coast of Scotland are interpreted as an evidence of a tsunami, probably generated by submarine slides occurring on the Norwegian continental slope around 7000 BP. If the slide caused tsunamis of such a magnitude as indicated by Dawson et al. and Long et al., then the coast of western Norway must also have been affected. Svendsen and Mangerud (1990) describe two sites south of Ålesund with possible tsunami deposits. In the first place sand layers with marine influence are interbedded in the lower part of the Holocene lacustrine gyttja. The threshold of this basin is 4 m above the Tapes transgression maximum. In the second place, situated 5 m above the Tapes level, and 6 m above the 7000 BP level, a disturbed layer including terrestrial turf is apparently the result of slumping triggered by an external source such as a tsunami.

It is of interest to calculate the run-up heights generated by one of the World's largest known submarine slides, which occurred in the Storegga area on the continental shelf off the coast of Møre, Mid-Norway, and compare these with the possible tsunami wave heights deduced from the geological evidences mentioned above. The calculations are also of interest in view of coastal activity and the large number of off-shore oil installations in the Nordic Seas.

Edgers and Karlsrud (1982) report that submarine slides might be triggered on slopes with an inclination less than 1°, and comprise enormous volumes in comparison to most terrestrial slides. They also report submarine slide velocities of 20-30 m/s, based upon the sequence of downslope cable breaks on Grand Banks, Newfoundland, in 1929.

Tsunamis are intermediate between tides and ripples in the spectrum of gravity water waves, with periods between 2 and 200 min, and with an initial surface elevation above the tsunami source of the order of one meter (Voit, 1987). From the studies on tsunamis by Hammack (1973) it is known that

the wave structure for relatively slow bed motions, as for submarine slides, is strongly dependent on the time-displacement history of the movement.

1.2 Geological data

The subsequent geological information is taken from the descriptions by Bugge et al. (1987,1988) and Jansen et al. (1987).

The Storegga ('great-edge') slide involved a total of about 5580 km^3 of sediment. The 290 km long headwall is located at the shelf edge 100 km off the coast. The slide scar, which covers an area of 34000 km^2, extends down-slope for 200-250 km, narrowing slightly towards the depositional area at the base of the continental slope below 2700 m. Slide deposits have been mapped for a further 500-550 km beyond this point. The total run-out distance could therefore be more than 750 km. The present maximum thickness of the deposits is 450 m. The average gradient of the whole slide scar is about 0.5°. The slope of the surface of the depositional area to the northwest is about 0.1°.

The available data indicate that the Storegga Slide was formed by three major events. The First Slide event probably occurred 30.000-50.000 years BP, and comprised the whole 290 km wide slide scar. The volume of this slide was about 3880 km^3, deposited both within and beyond the slide scar, i.e. 350-400 km from the headwall. The average thickness of the slide was about 114 m.

The Second Slide took place in the central part of the slide scar about 6000-8000 years BP. The slide cut deeper into the seabed and probably developed retrogressively, such that the headwall retreated 6-8 km onto the continental shelf, leaving the steep edge called Storegga. The slide travelled well out into the abyssal plain, probably more than 750 km from the headwall.

The Third Storegga Slide was limited to the upper part of the Second Slide scar, and probably occurred as a final, somewhat delayed stage of the Second Slide.

The volume of the last two slides was about 1700 km^3. This does not include any deposits of the First Slide removed by the later ones.

A partially liquified debris flow with enhanced pore water pressure was probably dominant in the First Slide, which mainly comprised poorly consolidated, soft clayey sediments. During the Second and Third slides (involving more consolidated sediments) the sliding sediments probably flowed down the gentle slope (as low as 0.1°) on liquified layers where excess pore pressure allowed the layers to act as lubricants. Turbidites, resulting mainly from the Second Slide, are also widely recognized through the immediate slide area, and a very thick distal turbidite found in the Norway basin 750 km from the headwall is related to the Second Slide.

The seismic activity in the area suggests that the primary triggering mechanism was earthquakes, perhaps in association with ice loading (for the First Slide) and the presence of gas and gas hydrates and excess pore water pressure.

Since the available information about volume, extension and run-out distance is most reliable for the First Storegga Slide, simulations are presented for this event only. As the First Slide comprised the biggest volume, it presumably generated the highest waves. However, the Second Slide redistributed a considerable portion of the First Slide deposits in addition to the above mentioned 1700 km^3. Hence the wave heights generated by the First and Second Slides did probably not differ considerably. The spatial relative variation of wave intensity and run-up heights revealed by the simulations were the same for both events.

2 Hydrodynamic equations

Waves generated by landslides in fjords of western Norway have been successfully simulated by a numerical model, Harbitz et al. (1991). The simulations presented herein are based on the same model, except for modifications due to a completely submarine slide motion starting from rest.

Gross features of the primary wave leaving the wave generation area may be determined for a submarine slide when the magnitudes of parameters which characterize the bed displacement are known. This was first done by Hammack (1973), who used the results to derive a scaled set of equations for tsunamis. By means of this scaled set, Ichiye (1983) gives criteria for

the linear long wave assumptions to be valid, based on the parameters which characterize the bed displacement. With slide dimensions and time scale as proposed in sec.4.3, we find that these criteria will be fulfilled also within the wave generation region for the Storegga Slide. Furthermore we find the wave lengths to be much less than the Rossby radius of deformation. Hence we do not expect the waves generated by the Storegga Slide to be substantially influenced by Coriolis' effects.

The equations are formulated in a Cartesian coordinate system with horizontal axes, Ox and Oy in the undisturbed water level and the vertical axis, Oz, pointing upwards. The fluid is confined to $-h < z < \eta$ where h is the depth referred to the datum $z = 0$, η the water surface displacement and we denote the total water depth by $H = h + \eta$. Since the slide introduces bathymetric changes, h will be a function of time (t). In terms of the averaged horizontal velocity, $\vec{u} = u\vec{i} + v\vec{j}$, where $\vec{i}$ and $\vec{j}$ denote the unit vectors in the x- and y-directions respectively, we obtain a linearized continuity equation of the form:

$$\frac{\partial H}{\partial t} = -\nabla \cdot (h\vec{u}) \tag{1}$$

Provided the pressure is hydrostatic and the nonlinear terms can be neglected the momentum equation becomes:

$$\frac{\partial \vec{u}}{\partial t} = -g\nabla\eta + \frac{\vec{\tau}}{\rho h} \tag{2}$$

where g is the acceleration of gravity, ρ is the density of the fluid and $\vec{\tau}$ is the bottom shear stress. The relative errors introduced are described in Harbitz et al. (1991, sec.2.1).

The equations are solved numerically by a finite difference technique. For the Storegga Slide event we will consider the influence of $\vec{\tau}$ (see sec.4.2). The implementation of this term is made by first computing the velocity components $u_{i+\frac{1}{2},j}^{n+\frac{1}{2}}$ and $v_{i,j+\frac{1}{2}}^{n+\frac{1}{2}}$ with $\vec{\tau}$ omitted. Subsequently the terms $[\tau_x \Delta t/(\rho \overline{h}^x)]_{i+\frac{1}{2},j}^{n+\frac{1}{2}}$ and $[\tau_y \Delta t/(\rho \overline{h}^y)]_{i,j+\frac{1}{2}}^{n+\frac{1}{2}}$ are added to $u_{i+\frac{1}{2},j}^{n+\frac{1}{2}}$ and $v_{i,j+\frac{1}{2}}^{n+\frac{1}{2}}$ respectively. The explicit expression for $\vec{\tau} = \tau_x \vec{i} + \tau_y \vec{j}$ is given by eq.(8). $f_{\beta,\gamma}^{\kappa}$ denotes the numerical approximation to a parameter f at a grid-point with coordinates $(\beta\Delta x, \gamma\Delta y, \kappa\Delta t)$ where Δx, Δy and Δt are the grid increments. For further details see Harbitz et al. (1991).

3 The slide model

The process of water wave generation by slides is found to be controlled by the global characteristics of the slide, Harbitz et al. (1991, sec.3). We shall therefore focus only on the total water displacement and the shear stress acting between the slide masses and the fluid.

The total water displacement is determined by the aggregated displacement thickness of the slide. The slide will therefore be described as one body with a prescribed motion. This corresponds to a time dependent water depth

$$h(x, y, t) = h_0(x, y) - h_s(x - x_s(t), y - y_s(t)) \tag{3}$$

where $h_0(x, y)$ represents the rigid sea floor, and h_s describes the water displacement by the slide body. By assuming a simple functional relation for the slide motion, the coordinates $(x_s(t), y_s(t))$ defined by

$$\left. \begin{aligned} x_s &= x_0 + \{\tfrac{1}{2}R(1 - \cos \tfrac{\pi t}{T})\} \cos \varphi \\ y_s &= y_0 + \{\tfrac{1}{2}R(1 - \cos \tfrac{\pi t}{T})\} \sin \varphi \end{aligned} \right\} \quad 0 < t < T \tag{4}$$

specify the motion of the slide. φ is the angle between the propagation direction of the slide and the x-axis. (x_0, y_0) is the position of the front of the slide when the movement starts ($t = 0.0 \ s$). R is the total horizontal displacement during the time interval T. We shall refer to R as the frontal run-out distance and to T as the running time of the slide. The maximum velocity of the slide is U_{max} and from eq.(4) we have

$$T = \frac{\pi}{2} \frac{R}{U_{max}} \tag{5}$$

The velocity profile of the slide will be discussed further in sec.4.1.

The shape of the slide is represented by a box form of length L, width B and maximum thickness Δh. To avoid sharp gradients in h, the edges of the box form is smoothed along both sides over a distance equal to B from the central line, and in the front and rear end over a distance S, by an exponential function of the form

$$h_s = \begin{cases} \Delta h \exp\left(-(2\frac{x'+S+L}{S})^4 - (2\frac{y'}{B})^4\right) & -(L+2S) < x' < -(L+S) \\ \Delta h \exp\left(-(2\frac{y'}{B})^4\right) & -(L+S) \le x' < -S \\ \Delta h \exp\left(-(2\frac{x'+S}{S})^4 - (2\frac{y'}{B})^4\right) & -S \le x' < 0 \end{cases} \tag{6}$$

6

where

$$x' = (x - x_s)\cos\varphi + (y - y_s)\sin\varphi$$
$$y' = - (x - x_s)\sin\varphi + (y - y_s)\cos\varphi$$

The x'-axis is directed along the direction of the slide motion, and the y'-axis in the transverse direction, with the origin in the front of the slide (confer Harbitz et al., 1991, fig.3).

The width of the slide, B, and the total length of the slide, $L + S$, constitutes the width of that part of the box which is thicker than $0.37 \cdot \Delta h$. With this definition of h_s the slide volume V is

$$V = 0.90B\Delta h(L + 0.90S) \tag{7}$$

where the factor 0.90 arises due to the smoothening.

The bottom shear stress acting on the water is expressed by

$$\vec{\tau} = \frac{1}{2}c_D^u\rho[(\dot{x}_s - u)^2 + (\dot{y}_s - v)^2]^{\frac{1}{2}} [(\dot{x}_s - u)\vec{\imath} + (\dot{y}_s - v)\vec{\jmath}] \tag{8}$$

where c_D^u is the drag coefficient (the dot denotes differentiating with respect to t).

i

4 The First Storegga Slide

4.1 The slide motion

Edgers and Karlsrud (1982) points out that geological evidence of submarine soil flows, in which the slide debris moves as a more or less concentrated fluid, has been found in a number of areas. Turbidity currents were previously emphasized as the predominant mechanism in very large and rapid submarine slides. However, Edgers and Karlsrud find it difficult to see how the main body of a flowing mass will become sufficiently dilute to turn into a low density current. The viscous flow analysis of slide run-out velocity by the same authors (Edgers and Karlsrud 1981), provides good agreement with available field observations. For the back calculated soil viscosities, the Reynolds number indicates laminar conditions at the soil/water interface. This precludes the large amount of turbulent mixing necessary to maintain the flow

primarily as a turbidity current. The soil viscosities also agree remarkably with viscosities of clearly viscous sub-aerial quick clay slides.

The tangential gradient of the slide thickness is assumed to be small (as for the Storegga Slides). The resultant active pressure acting on one single element of the slide from the neighbouring elements will therefore be small compared to gravitational forces (see Norem et al., 1989). This suggests a rigid body description of the slide. As long as the dense flow is accelerating, it will not be surpassed by a turbidity current generated by the initial slides.

The internal velocity gradient normal to the slope will also be small for a submarine flowslide with dimensions like the Storegga Slides. Hence viscous shear stresses are of importance only on the upper surface and along the base of the slide. The viscous shear stresses are described by a dynamic drag proportional to the slide velocity squared. As the slide consists of blocks that slide and bounce, the resistive forces along the base of the slide should also include a Coulomb friction term. Wave energy considerations have revealed that the contribution to the total wave energy from displacement effects clearly exceeds the contribution from shear stress effects, especially in the initial stages of the slide motion. Hence a wave resistance must be included in the forces acting upon the slide.

The slide velocity U for a slide moving on a linear slope with inclination angle α, assuming that there is no mass entrainment along the path, is consequently determined by the momentum equation

$$\frac{dU}{dt} = \frac{\bar{\rho} - \rho_t}{\bar{\rho}} g(\sin\alpha - \mu\cos\alpha) - \frac{1}{2}(c_D^u + c_D^b)\frac{\rho_t}{\bar{\rho}\bar{h}}U^2 - \frac{R_w}{\bar{\rho}\bar{h}} \qquad (9)$$

where $\bar{\rho}$ is the average density of the slide masses, ρ_t is the density of the turbidity current surrounding the slide masses, $\bar{h}$ is the average thickness of the slide and R_w is the wave resistance per unit area. c_D^u and c_D^b are the drag coefficients along the upper surface and along the base of the slide respectively and μ is the Coulomb friction coefficient.

For a numerical solution R_w can be found by integrating the pressure along the surface of the slide at each time step. Following Norem et al. (1989) the value of c_D^u averaged over the slide length $L + S = 225$ km, for turbulent flow along a flat rough plate moving with slowly varying velocity,

is defined through the equation proposed by Schlichting (1968)

$$c_D^u = [1.89 + 1.62 \log \frac{(L+S)}{k}]^{-\frac{5}{2}} \tag{10}$$

where k is a roughness length in the range 0.01-0.1 m. Hence c_D^u will be between 0.0014 and 0.0019. The upper value is selected for the simulations in sec.4.3. There is uncertainty connected to the values of all parameters appearing in eq.(9), as well as to possible mass entrainment. The parameters can not be determined exactly by core samples from the slide deposits, as the present structure is significantly altered from when the slide was moving. Samples of the materials deposited by the First Storegga Slide don't even exist (Jansen, 1987). Thus predictions of the velocities of the Storegga Slides will never be more than very rough estimates, even though the main contributing physical effects are included.

If the wave resistance is ignored and the friction and drag coefficients are considered to be constants, the terminal slide velocity is expressed by

$$U_{term} = \sqrt{\frac{(\bar{\rho} - \rho_t)g\bar{h}(\sin \alpha - \mu \cos \alpha)}{\frac{1}{2}(c_D^u + c_D^b)\rho_t}} \tag{11}$$

Excess pore pressure will reduce the Coulomb friction coefficient significantly. For a slide scar with inclination angle $\alpha = 0.5°$, μ is determined by $\tan 0.5° > \mu > \tan 0.1°$ (the inclination angle of the depositional area). An average value of 0.005 is selected. Finally ignoring the viscous drag along the base of the slide ($c_D^b = 0.0$), the terminal slide velocity U_{term} is estimated to 48.9 m/s for a slide flowing on an infinite path length with parameter values as given in table 1. The terminal slide velocity will be reduced if a viscous drag along the base is included. The wave resistance will initially reduce the slide velocity. Since the slide motion is clearly sub-critical (i.e. $U_{max}/\sqrt{g\bar{h}} < 1$), the primary waves, mainly caused by displacement effects during the early stages of the slide motion, will advance faster than the slide and leave the slide area, and it may easily be shown that for a slide moving with slowly varying velocity on a slowly varying seabed (as is the case during the following stages of the slide motion), the wave resistance due to displacement effects will be negligible. In this case the waves generated by shear stress effects will cause a negative wave resistance (confer the analytical solutions by Harbitz

9

Table 1: Parameter values used to determine terminal slide velocity.

α	inclination angle of slope	0.5 °
$\bar{\rho}$	average density of slide masses	$1.7 \cdot 10^3$ kg/m^3
ρ_t	density of turbidity current	$1.1 \cdot 10^3$ kg/m^3
$\bar{h}$	average thickness of slide	114.0 m
μ	Coulomb friction coefficient	$5 \cdot 10^{-3}$
c_D^u	drag coefficient	$1.9 \cdot 10^{-3}$

et al., 1991), which will again increase the slide velocity. In the subsequent analysis, $U_{max} = 50.0$ m/s will be applied as an absolute upper limit of the maximum slide velocity.

For the 1929 Grand Banks Slide, Newfoundland, which comprised 760 km^3 and travelled on a slope with depth profile comparable with the Storegga one, a sequence of downslope cable breaks revealed slide velocities of 20-30 m/s within the first 100-200 km of the run-out distance (Edgers and Karlsrud, 1982). $U_{max} = 20.0$ m/s will therefore be applied as a lower limit of the maximum slide velocity, while an intermediate value of 35.0 m/s will be applied as the most likely maximum velocity of the slide. The general observation referred by Edgers and Karlsrud (1982) that the ratio of total run-out distance to total height difference increases with the volume of submarine slides, supports the choice of a somewhat higher maximum velocity for the Storegga Slide than for the Grand Banks Slide.

With the same limitations and parameter values as used to determine the terminal slide velocity, a velocity of 35 m/s is reached when the slide has travelled approximately a distance $R/2 = 75.0$ km, which is less than the distance for the gravity centre of the slide to reach the depositional area where the slope is less than 1°. If this was not the case, the retardation would have started before the slide obtained a velocity of 35 m/s.

By simulations with different variation of the slide velocity in time, i.e. different velocity profiles of the slide motion, it is established that the form of the velocity profile during the retardation phase of the slide is of minor importance. This is a consequence of the sub-critical slide motion, and sup-

ports the choice of the most simple curve reproducing both an acceleration phase and a retardation phase of the slide, given by eq.(4). Simulations also reveal that the wave heights increase significantly with the acceleration of the slide. The velocity profile defined by eq.(4) with $U_{max} = 35.0$ m/s and $R = 150.0$ km approximately reproduces the initial acceleration defined by eq.(9) with the same limitations and parameter values as used to find U_{term} (the viscous drag is anyhow initially negligible). Simultaneously the slide reaches a velocity of 35.0 m/s when the slide has travelled a distance $R/2$. Thus we consider this velocity profile to represent an estimate as good as any during the acceleration phase of the slide. The velocity profile is depicted in fig.3. $U(t)$ is here defined as $| \dot{x}_s \vec{i} + \dot{y}_s \vec{j} |$.

To demonstrate the significance of the velocity profile, the wave heights generated with velocity profiles defined by eq.(4) with $U_{max} = 20.0$ m/s and $U_{max} = 50.0$ m/s ($R = 150.0$ km), fig.3, will also be presented in sec.4.3.

The initial acceleration of the slide defined by eq.(4) is 0.005 m/s^2 and 0.033 m/s^2 with $U_{max} = 20$ m/s and $U_{max} = 50$ m/s respectively. Simulations with $U_{max} = 35$ m/s, but with other velocity profiles than defined by eq.(4), reveal wave heights between the results obtained with $U_{max} = 20$ m/s and $U_{max} = 50$ m/s in eq.(4), as long as the initial accelaration of the slide is between the two values mentioned above. Hence the wave heights resulting from the latter profiles are assumed to represent the absolute upper and lower limits of the wave heights generated by the First Storegga Slide.

4.2   Effects of shear stress on the fluid/slide interface

In order to estimate the effect of shear stress on the wave height, we shall use the analytical solutions discussed by Harbitz et al. (1991). If η^τ_{max} and η^d_{max} denote the maximum surface elevation due to bottom shear stress and volume displacement respectively, we have $\frac{\eta^\tau_{max}}{\eta^d_{max}} = c^u_D \frac{U/\sqrt{gh_0}(L+S)}{2\Delta h}$, for a two-dimensional slide with total length $L + S$ and maximum thickness Δh moving on a horizontal bottom at depth h_0 with constant velocity U. The bottom shear stress is here expressed by $\tau = \frac{1}{2}c^u_D \rho U^2$. With $L + S = 225.0$ km, $\Delta h = 114.0$ m (as the First Storegga Slide), $h_0 = 2700.0$ m, $U = 35.0$ m/s and $c^u_D = 0.0019$, we find $\frac{\eta^\tau_{max}}{\eta^d_{max}} = 0.4$. This implies that the effects of

11

Table 2: Parameters for slide volume and path of slide motion.

L	length of the slide	150.0	km
B	width of the slide	175.0	km
S	smoothing distance, front and rear end	75.0	km
Δh	height of the slide	114.0	m
φ	direction of the slide motion relative to the x-axis	174.9	°
R	frontal run-out distance	150.0	km

shear stress at the interface between the water and the slide body can not be neglected when considering the wave formation ascribed to the Storegga Slide, as confirmed by the results referred in table 3. Hence the effect of the bottom shear stress is included in the numerical simulations.

4.3   The simulated wave structure

The model domain with coordinate axes, initial location of the slide and the location of the eight stations where we analyse time series of the surface elevation, are shown in fig.1. The depth profile for the slide area is shown in fig.2. Estimated values of the slide parameters, based on the information in sec.1.2, are listed in table 2. The model domain constitutes 192 × 220 grid cells. The grid increments are $\Delta x = \Delta y = 12.5$ km. The depth matrix is based on the present bathymetry of the Nordic Seas. Even though bathymetric changes due to reduced ice loading and crustal motions have occurred, the difference between the present water level and the water level at the time of the sand layer deposition (7000 yrs. BP), is only of the order of 10 m along the coast of western Norway, Sørensen et al. (1987). At the locations inside point 8, eastern coast of Scotland, the corresponding difference is less than 6 m, Long et al. (1989). These differences may only slightly affect the wave propagation in shallow water regions. In deep sea regions, including the wave generation area, the effect of water level changes is insignificant. Thus we expect the applied depth matrix to be appropriate in spite of the water level changes.

Table 3: Maximum and minimum values of sea surface displacement for U_{max} = 20, 35, 50 m/s, as well as explicit values of η^d and η^τ for U_{max} = 35.0 m/s, in stations (1-8).

		station no.							
		1	2	3	4	5	6	7	8
$U_{max} = 20.0\ m/s$	$\eta_{max}\ (m)$	1.4	0.9	1.8	2.9	2.6	1.5	2.0	1.2
	η_{min}	-1.1	-1.1	-1.7	-4.7	-2.3	-2.9	-2.8	-1.8
$U_{max} = 35.0\ m/s$	η_{max}	5.1	3.6	7.0	10.5	5.6	7.1	4.8	3.5
	η_{min}	-6.9	-3.3	-5.9	-11.6	-8.1	-5.4	-5.5	-4.1
	η^τ_{max}	2.4	1.8	2.4	2.9	2.7	1.1	1.9	1.3
	η^τ_{min}	-2.1	-0.7	-1.5	-6.1	-2.6	-2.8	-3.0	-2.2
	η^d_{max}	4.0	2.9	5.8	12.0	4.7	8.3	5.7	4.0
	η^d_{min}	-7.1	-3.4	-6.7	-9.9	-7.6	-4.0	-3.9	-3.5
$U_{max} = 50.0\ m/s$	η_{max}	12.4	8.8	13.6	12.4	13.1	13.0	6.7	4.9
	η_{min}	-17.7	-8.9	-14.2	-19.1	-12.9	-10.6	-7.0	-6.4

The significance of the velocity profile will in accordance with the discussion in sec.4.1, be demonstrated by setting maximum slide velocity U_{max} = 20.0, 35.0 and 50.0 m/s in the profile defined by eq.(4), see fig.3. The extremes of the sea surface displacement at the eight stations are referred in table 3. In order to compare η^τ and η^d, the values have been calculated separately for U_{max} = 35.0 m/s (by choosing c_D^u = 0.0019, Δh = 0.0 m, i.e. no volume displacement, for η^τ, and c_D^u = 0.000, Δh = 114.0 m for η^d). Fig.4 shows the complete time series of η for U_{max} = 35.0 m/s. A secondary wave of 7.1 m in station 6 would probably not occur with open boundary conditions along the boundaries of the computational domain located at sea.

For relatively slow submarine slide motion, the height of the primary wave increases approximately in proportion to the velocity of the slide, given by U_{max}, for a fixed value of T. In this case we will from eq.(4) find the initial acceleration of the slide to be proportional to U_{max} for $t \ll T$. For real slide events the value of R can often be estimated, as for the First Storegga

Slide. With R fixed, the value of T will have to decrease while U_{max} is increased. Hence the initial acceleration of the slide will be proportional to U_{max}^2 for $t \ll T$. This explains why the height of the primary wave seems to be approximately proportional to U_{max}^2 rather than U_{max}, as indicated by the results in table 3. In fact it may be deduced from eq.(1) that the surface elevation initially increases in time in proportion to U_{max}^2. The validity of the results is therefore strongly dependent on a correct estimate of the maximum slide velocity.

The simulated wave pattern for $U_{max} = 35.0$ m/s is shown in fig.5-9. The sea surface displacement introduced by the slide appears at t=1.0 hour as a characteristic, symmetric wave pattern consisting of a sickle shaped surface elevation with a maximum height of about 3 m, followed by a surface depression with a minimum height of about -15 m, fig.5-6. At t=2.0 hours, the primary wave has reached the eastern coast of Iceland, and the wave height outside the shore is about 5 m, fig.7-8. Simultaneously there is a wave strongly affected by refraction, possibly an edge wave, propagating northwards along the Norwegian coast with its crest approximately perpendicular to shore line. At t=3.0 hours, the wave height east of Greenland is about 5 m, while the wave height north of Scotland is 1.5 m only, fig.9. We conclude that most of the wave energy induced by the slide propagates towards Greenland and Iceland, rather than Scotland.

4.4   Estimated run-up heights

Waves approaching the shore line will amplify and wash up the beach slope. By the method described by Harbitz et al. (1991, appendix) rough estimates for the maximum run-up height may be found from the calculated height η^p and the period T^p of the primary waves at stations off the coast of Greenland, Iceland and Scotland (insignificant precursors in stations 7 and 8 are disregarded). The final amplification is assumed to take place along a linear slope with inclination angle θ between the point of depth h_0 where η^p is read, and the shore line. The periods of the incident waves are estimated directly from the time series. Values for the run-up computation are presented in table 4. An estimate of the run-up height inside station 7 is omitted due to the

critical location outside Moray Firth. The beach slopes of this estuary are exposed for significant run-up heights which can only be found by a detailed analysis including local effects.

Along the Norwegian coast a precursor with downward displacement of the sea surface occurred, as indicated by the time series from station 4, fig.4. The time series together with the contour plot in fig.9 reveal that the subsequent positive sea surface displacement caused run-up heights of 10-15 m.

The estimated amplification factor for the waves between the stations where η^p is read and the shore line, varies from 1.1 to 2.5. Such small values are a direct consequence of the large wave lengths with corresponding wave periods much longer than normally reported in tsunami events. Where the continental shelf is narrow, landward propagating waves will experience the continental slope and the shore line almost as one vertical wall, causing the amplification factor between a station outside the continental shelf and the shore line to be approximately 2.

In the applied method for estimating run-up heights (Harbitz et al., 1991, appendix), the incident wave is replaced by a single periodic harmonic with period T^p and amplitude η^p. Normally the periodic wave in its entirety will reach higher than the primary wave alone. The difference between the run-up height for a single crested wave and for a single periodic wave is however small for long waves (see Pedersen, 1987). In station 8, eastern coast of Scotland, there will hardly be any difference at all, as the situation with a surface depression preceding the primary wave is more closely related to a periodic wave.

With $U_{max} = 35$ m/s, the run-up heights resulting from the First Storegga Slide, which represents a maximum of the run-up heights generated by all three events, slightly exceed the run-up heights from the Second Slide deduced by Dawson et al. (1988), recording that "the tsunami struck the eastern coast of Scotland and reached a height of at least 4 m above contemporary high water mark in some inlets". By reducing the maximum slide velocity to 20 m/s, the run-up heights are reduced to 1.8 m on the eastern coast of Iceland, and about 1.5 m on the eastern coast of Greenland and the coast of northern Scotland. A maximum slide velocity of 50 m/s reveals

Table 4: Estimated run-up heights, R^p, for primary wave. $U_{max} = 35.0$ m/s.

Locations	Stations	h_0 (m)	θ (deg)	T^p (h)	η^p (m)	R^p (m)
East Greenland	1	233	0.71	2.20	5.1	5.6
East Iceland	5	157	0.34	2.17	5.6	7.8
North Scotland	6	61	0.13	2.27	2.0	5.0
East Scotland	7	72	0.05	3.03	4.8	—
East Scotland	8	76	0.23	2.57	3.5	4.6

run-up heights of 21 m along the eastern coast of Iceland, 12.0 m along the eastern coast of Greenland and 13.3 and 6.9 m along the northern and eastern coast of Scotland respectively.

It should be emphasized that run-up heights may be significantly increased by local topographical effects causing resonance phenomena as well as interference, focusing or trapping of the incident waves (e.g. Liu, 1981). Traces of larger run-up heights resulting from these effects may possibly be found in a few peculiar places, but will not be recognizable in a larger region. Oblique angles of incidence as well as wave breaking will generally reduce the amplification.

In exposed areas traces of the tsunami might have been washed away by waves from regular storms. Tsunamis will however, like tidal waves, propagate for long distances into bays and fjord systems, and thereby leave well-defined traces in otherwise sheltered areas.

4.5 Some remarks on the numerical computations

The slide is assumed to move upon the existing sea bed, i.e. upon the real slide deposits. The error introduced by this simplification will be small since the thickness of the deposits and the moving slide is relatively small compared to the water depth. The effect of a retrogressive slide movement is omitted. This is probably more important for the Second and Third Storegga Slides, and will by no means affect the primary outward propagating wave.

As stated above, tsunamis are not influenced by Coriolis' effects. However, it should not be concealed that these effects might originate Kelvin waves where the width of the continental shelf is at least 300 km. If such waves arose, they slightly affected the wave heights in the coastal areas.

The exponential smoothing function, eq.(6), is favoured because little high frequency numerical noise is introduced compared to other smoothing functions. A reduced smoothing distance S will introduce more high frequency noise, and increase the steepness of the primary wave. However, the main characteristics and the wave heights are approximately unchanged as long as the total slide volume is kept constant.

5 Conclusions

Wave run-up heights generated by the Storegga Slides are computed on the basis of a numerical model. Since the available information about volume, extension and run-out distance is most reliable for the First Storegga Slide, simulations are presented for this event only. As the First Slide comprised the biggest volume, it presumably generated the highest waves. The volume removed by the Second Slide comprised about one half of the volume of the First Slide. However, the Second Slide redistributed a considerable portion of the First Slide deposits. Hence the wave heights generated by the First and Second Slides did probably not differ considerably, and the results are in remarkably good agreement with wave heights deduced from possible deposits of the Second Slide tsunami in northern Scotland, Dawson et al. (1988). The simulated wave heights along the western coast of Norway also support Svendsen and Mangerud's (1990) conjecture about tsunami deposits south of Ålesund.

The model is based on the linearized hydrostatic shallow water equations for wave propagation in open sea regions and a slide model for describing the dynamics of the slide body. The wave energy induced by the slide propagates mainly towards Greenland and Iceland (i.e. in the direction of the slide motion). The generated wave heights increase significantly with the acceleration of the slide. For a fixed run-out distance the selected velocity profile, i.e. the variation of the slide velocity in time, is determined simply by the maximum

slide velocity. A correct estimate of this parameter is therefore essential. The most likely maximum slide velocity of 35 m/s is estimated from considerations of a slide moving on a linear slope and from comparisons with recorded velocities of the submarine 1929 Grand Banks Slide, Newfoundland, Edgers and Karlsrud (1982).

Local wave amplification in the wave run-up zone are estimated by comparing results from an idealized numerical run-up model using a no-flux boundary condition with an analytical model for calculation of run-up heights on a gentle beach slope. The large scale run-up heights are found to be 7.8 m on the eastern coast of Iceland, 5.6 m on the eastern coast of Greenland and about 5 m on the coast of northern Scotland for a maximum slide velocity of 35 m/s. Along the Norwegian coast there was primarily a precursor with downward displacement. The subsequent positive sea surface displacement caused run-up heights exceeding 10 m. By reducing the maximum slide velocity to 20 m/s, the run-up heights are reduced to 1.8 m on the eastern coast of Iceland, and about 1.5 m on the eastern coast of Greenland and the coast of northern Scotland. A maximum slide velocity of 50 m/s reveals run-up heights of 21 m along the eastern coast of Iceland, 12.0 m along the eastern coast of Greenland and 13.3 and 6.9 m along the northern and eastern coast of Scotland respectively. The limited amplification is a direct consequence of the large wave lengths with corresponding wave periods much longer than normally reported in tsunami events.

In view of the predicted run-up heights, the eastern coast of Iceland and the western coast of Norway were most exposed to the tsunami. Traces of a tsunami are therefore most likely to be detected in these regions.

Analysis of the effects of shear stress at the interface between the water and the slide body, has proved that this effect must be included. Except for run-up zones with gentle beach slopes, the assumptions of linear long wave propagation are fulfilled in the entire computational domain.

Acknowledgements

tion.

References

[1] Bugge,T., Befring,S., Belderson,R.H., Eidvin,T., Jansen,E., Kenyon,N.H., Holtedahl,H. and Sejrup,H.P. 1987: A Giant Three-Stage Submarine Slide Off Norway. *Geo-Marine Letters* **7**, pp. 191-198.

[2] Bugge,T., Belderson,R.H. and Kenyon,N.H. 1988: The Storegga Slide. *Phil Trans. R. Soc. Lond.* A **325** (1988), pp. 357-388.

[3] Dawson,A.G., Long,D. and Smith,D.E. 1988: The Storegga Slides: Evidence from Eastern Scotland for a Possible Tsunami. *Marine Geology* **82**, pp. 271-276.

[4] Edgers,L. and Karlsrud,K. 1981: Viscous Analysis of Submarine Flows - Field Case Studies. *Norwegian Geotechnical Institute* Report **52207-8**.

[5] Edgers,L. and Karlsrud,K. 1982: Soil Flows Generated by Submarine Slides - Case Studies and Consequences. *Norwegian Geotechnical Institute* Publication no. **143**.

[6] Hammack,J.L. 1973: A Note on Tsunamis: Their Generation and Propagation in an Ocean of Uniform Depth. *J. Fluid Mech.* Vol. **60**, part 4, pp. 769-799.

[7] Harbitz,C., Pedersen,G. and Gjevik,B. 1991: Numerical Simulation of Large Water Waves Due to Landslides. *Preprint Series, Dep. of Mathematics, University of Oslo* No. **3**.

[8] Ichiye,T. 1983: Tsunami Gneration as Finite Depth Cauchy-Poisson Problem or Long Wave Problem. *Tsunamis - Their Science and Engineering*, edited by K.IIda and T.Iwasaki, pp.265-274.

[9] Jansen,E., Befring,S., Bugge,T., Eidvin,T., Holtedahl,H. and Sejrup,H.P. 1987: Large Submarine Slides on the Norwegian Continental Margin: Sediments, Transport and Timing. *Marine Geology* **78**, pp. 77-107.

[10] Liu,P.L.-F. 1981: Effects of the Continental Shelf on Harbor Resonance. *Tsunamis - Their Science and Engineering*, edited by K.IIda and T.Iwasaki, pp.303-314.

[11] Long,D., Smith,D.E. and Dawson,A.G. 1989: A Holocene Tsunami Deposit in Eastern Scotland. *Journal of Quaternary Science* 4, pp. 61-66.

[12] Norem,H., Locat,J. and Schieldrop,B. 1989: An Approach to the Physics and the Modelling of Submarine Flowslides. *Norwegian Geotechnical Institute* Report **522090-2**, Nov. 1989.

[13] Pedersen,G. 1987: Run-up of Cnoidal Waves. *Preprint Series, Dep. of Mathematics, University of Oslo* No. 4.

[14] Schlichting,H. 1968: Boundary Layer Theory. *McGraw Hill.*

[15] Sørensen,R., Bakkelid,S. and Torp,B. 1987: Landhevning (Land Uplift). *Nasjonalatlas for Norge* Kartblad (map sheet) **2.3.3**.

[16] Svendsen,J.I. and Mangerud,J. 1990: Sea-level changes and pollen stratigraphy on the outer coast of Sunnmøre, western Norway. *Norsk Geologisk Tidsskrift* Vol. **70**, pp. 111-134.

[17] Voit,S.S. 1987: Tsunamis. *Ann. Rev. Fluid Mech. 1987* **19**, pp. 217-236.

Figure captions

Figure 1:

Model domain on a stereographic map projection.

——: Initial location of the central line of the slide, − −: frontal run-out distance, ↑: northward direction from rear end of slide, (1 − 8): location of the 8 stations were time series of sea surface displacement are analysed.

Figure 2:

Depth profile in the slide area.

Figure 3:

Velocity profiles defined by eq.(4) (with $R = 150.0$ km).

Figure 4:

Simulated time series of sea surface displacement with $U_{max} = 35.0$ m/s, $Deltah = 114.0$ m and $c_D^u = 0.0019$.

Figure 5:

Simulated wave pattern at t=1 hour after the release of the slide for $U_{max} = 35.0$ m/s, $Deltah = 114.0$ m and $c_D^u = 0.0019$. Contour lines for wave height with interval 1.0 m. Solid lines indicate surface elevation. Maximum height of outward propagating primary wave: 3 m.

Figure 6:

Perspective view of sea surface displacement at t=1.0 hour after the release of the slide. Parameter values as in fig.5.

Figure 7:

Simulated wave pattern at t=2 hours after the release of the slide. Parameter values and contour line interval as in fig.5. Maximum height of wave approaching Iceland: 5 m.

Figure 8:

Perspective view of sea surface displacement at t=2.0 hours after the release of the slide. Parameter values as in fig.5.

Figure 9:

Simulated wave pattern at t=3 hours after the release of the slide. Parameter values and contour line interval as in fig.5. Maximum height of wave approaching Scotland: 1.5 m, Greenland: 5 m.
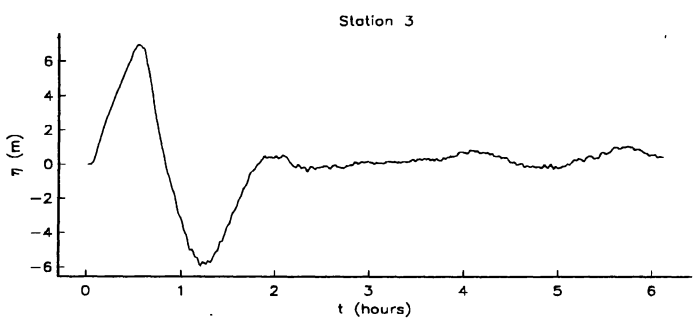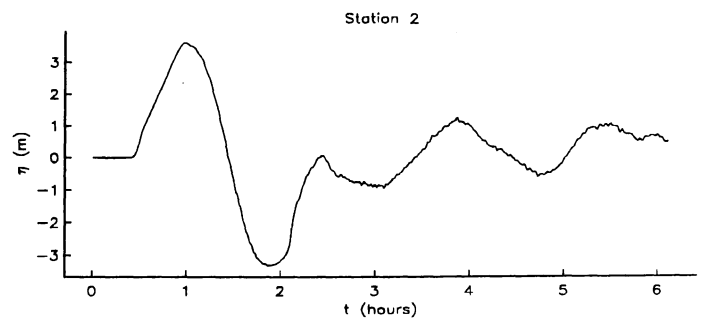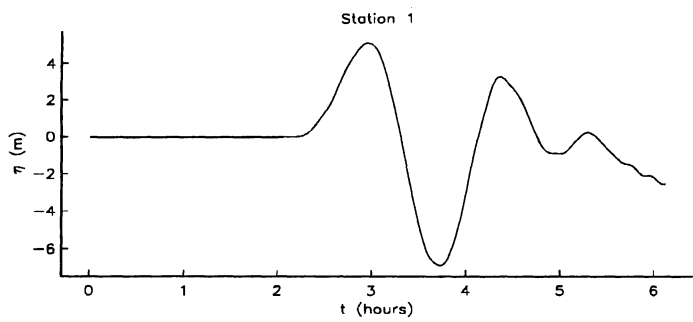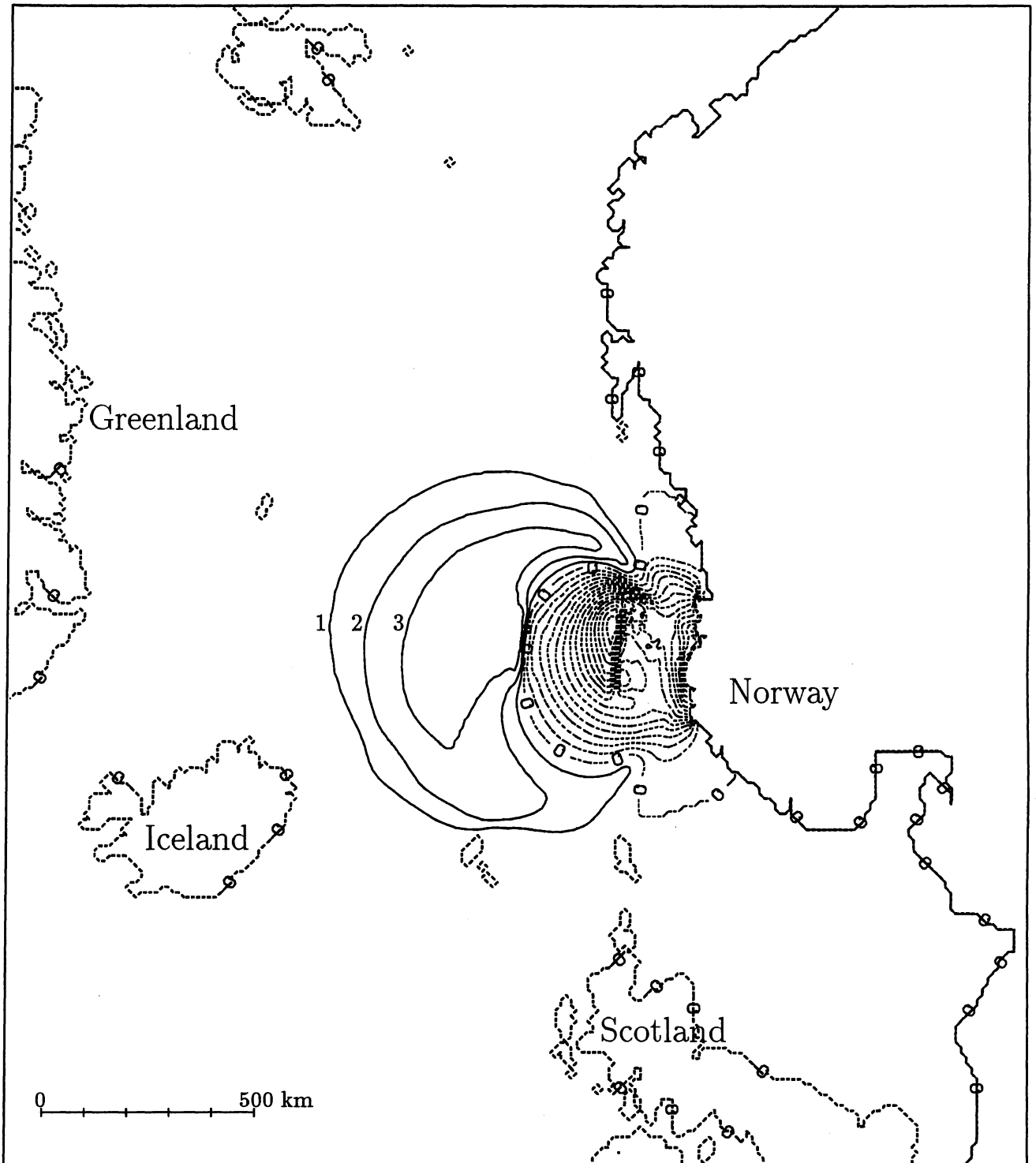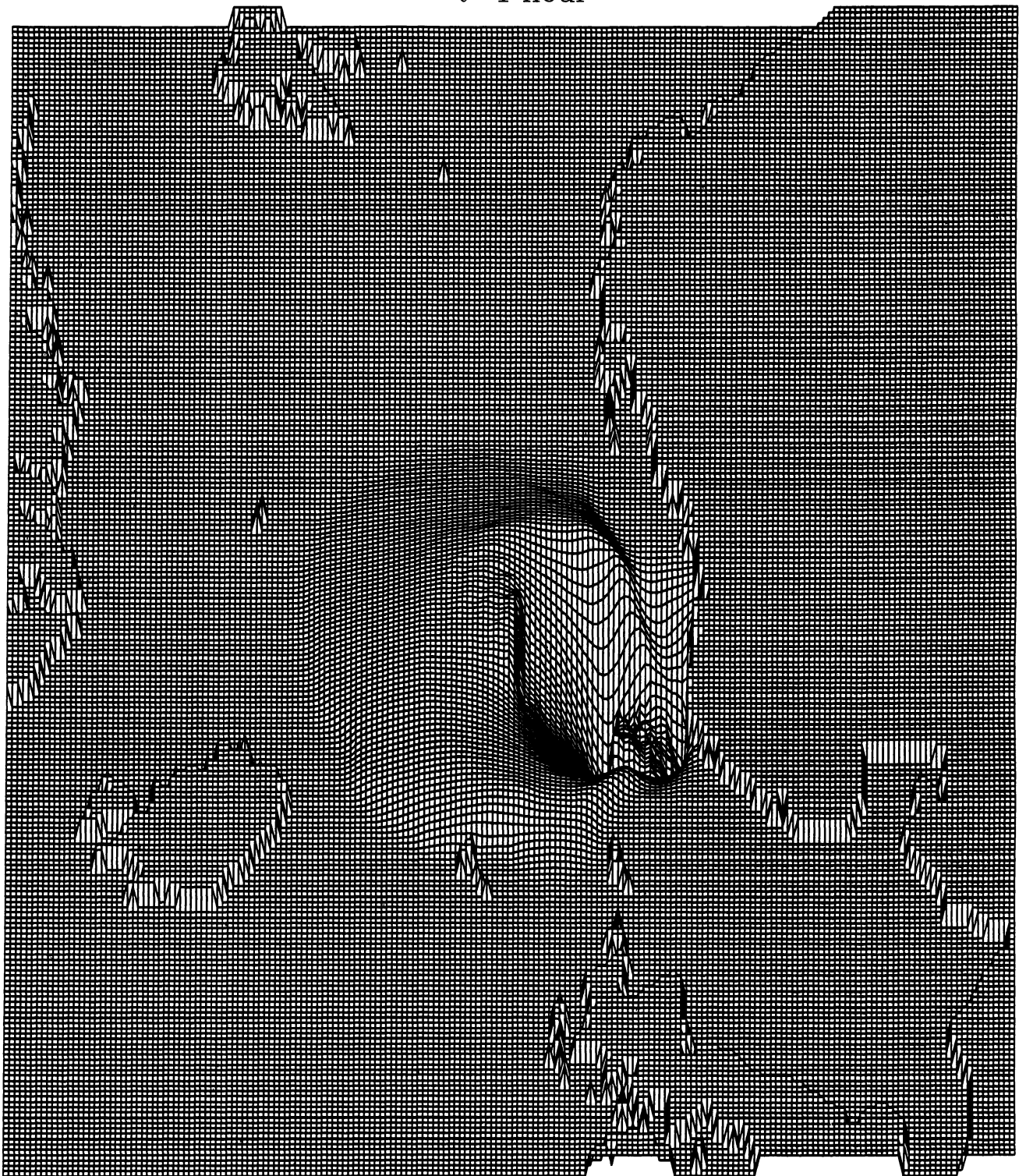
Figures
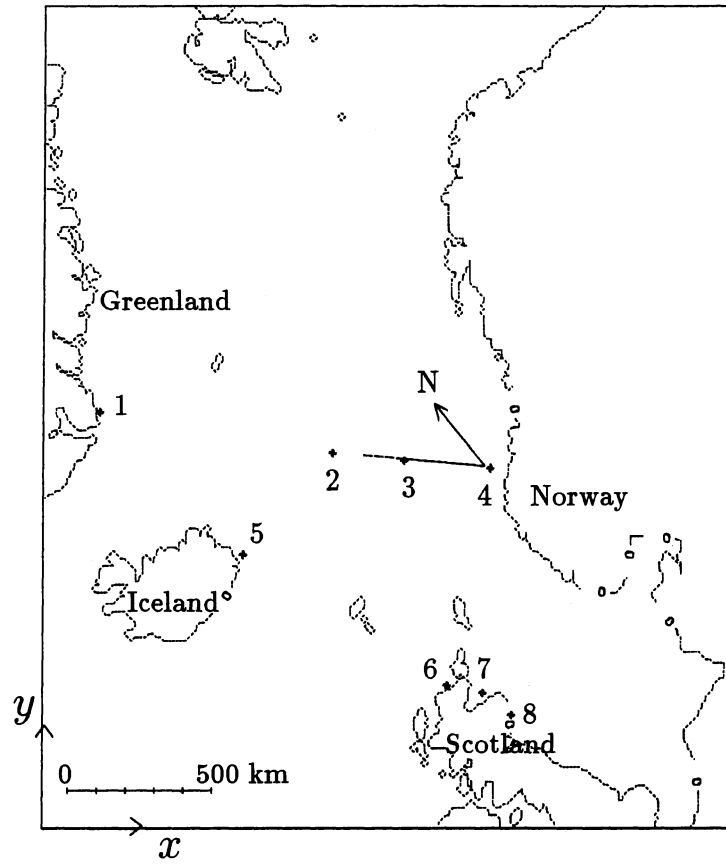
Figure 1:
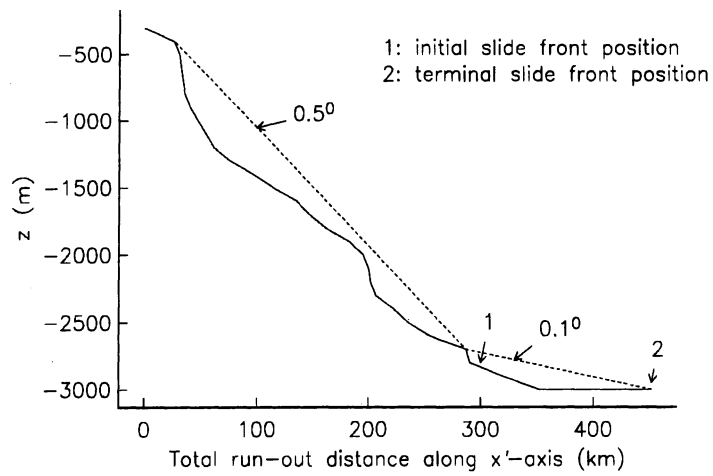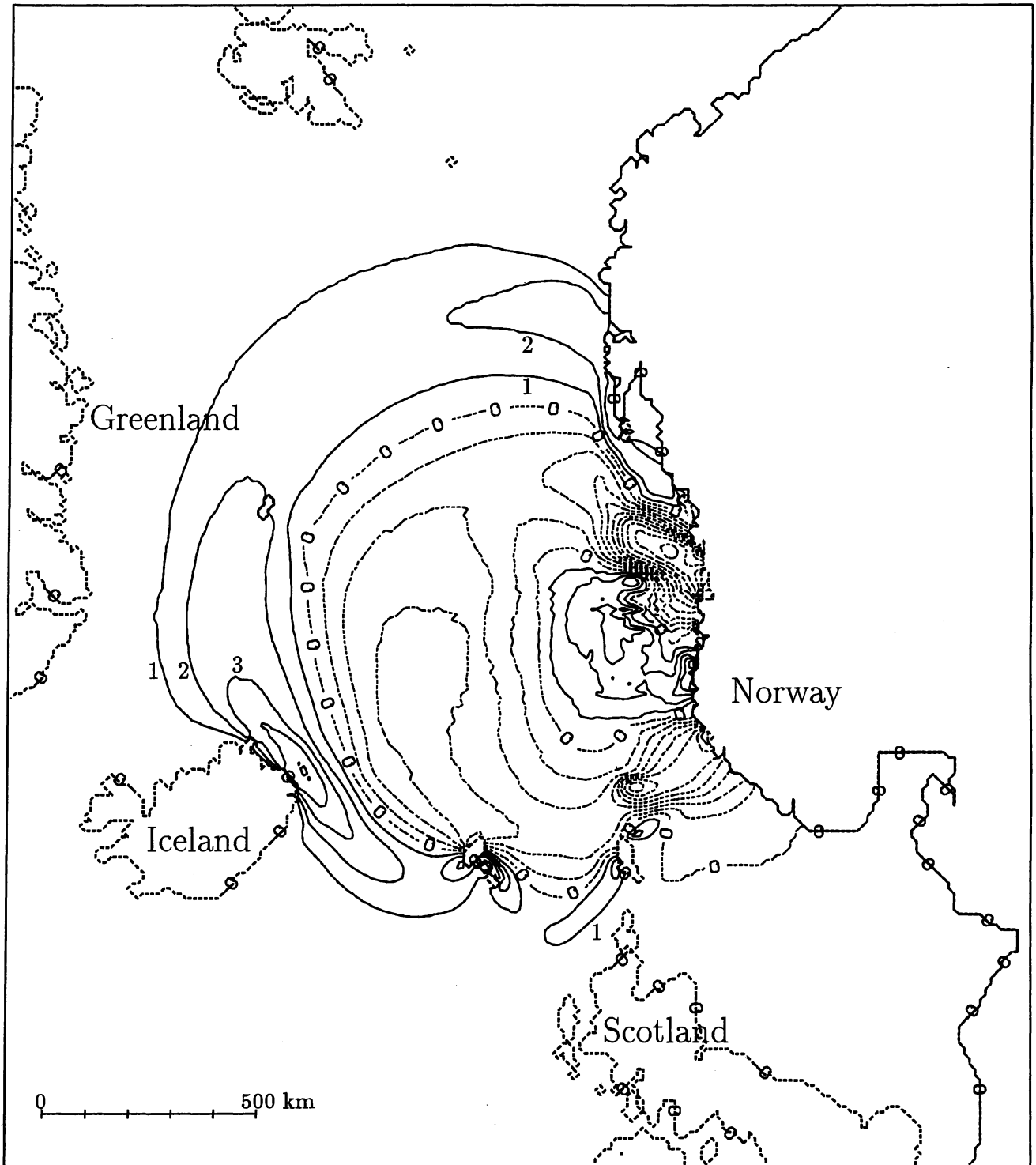

Figure 2:
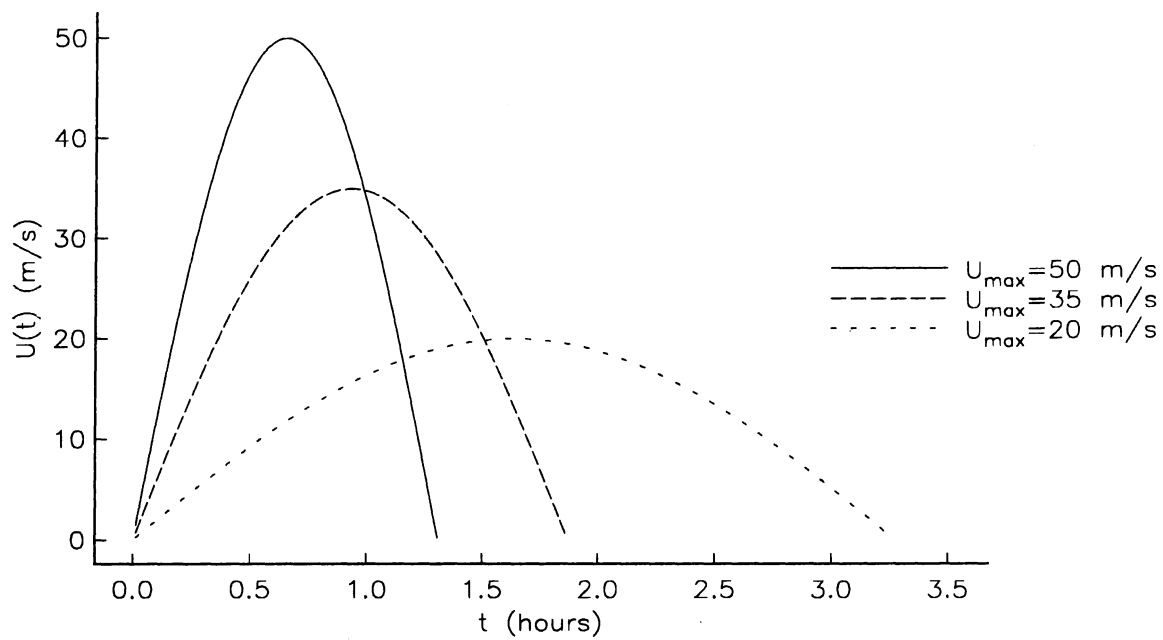
Figure 3:
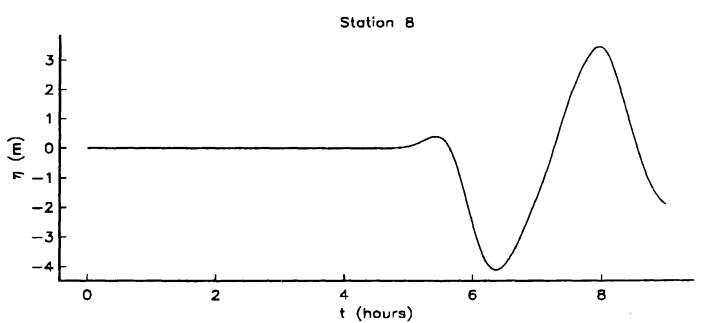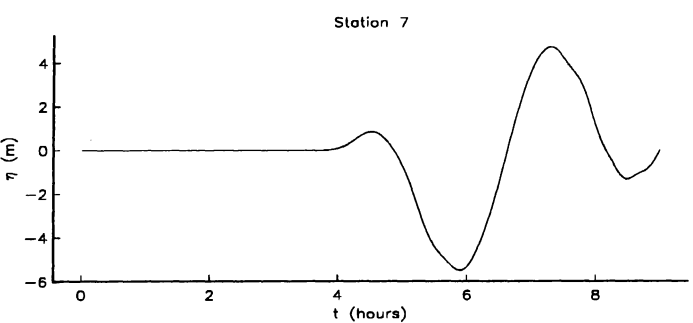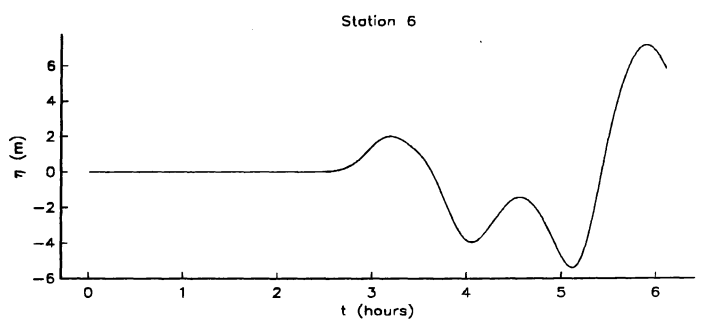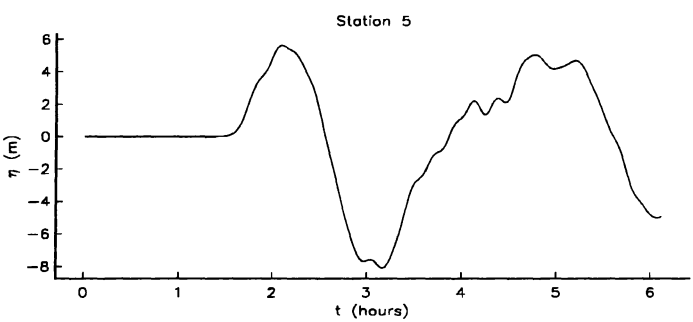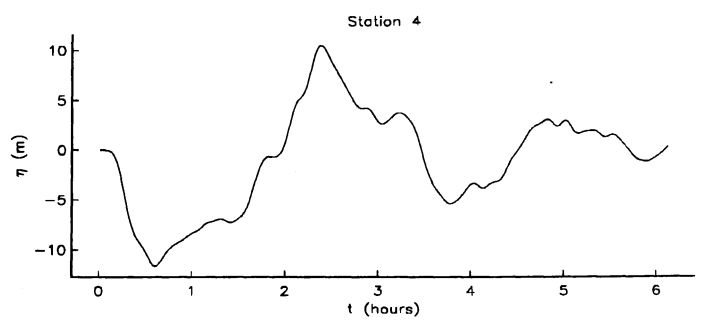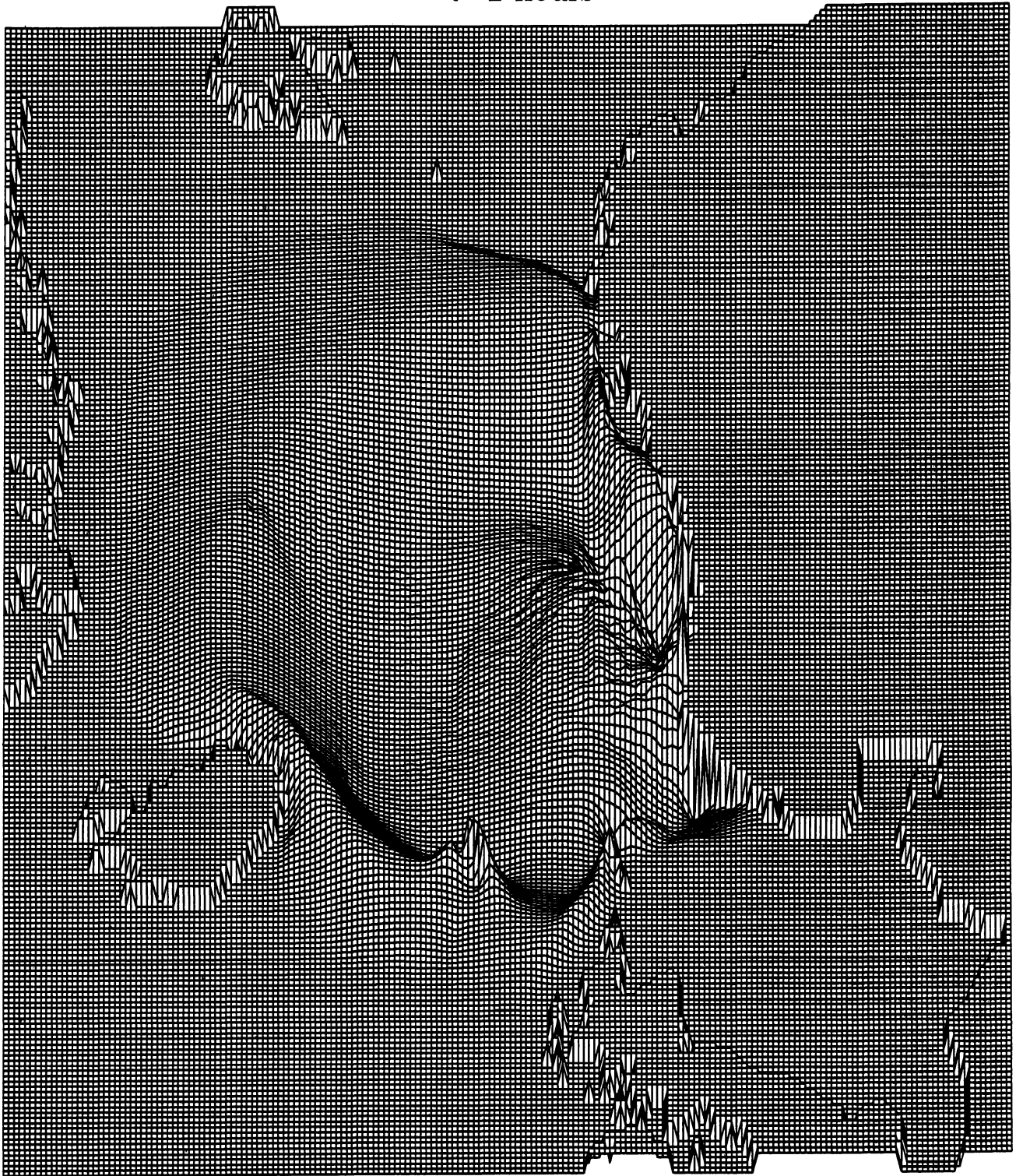
Figure 4:

Figure 5:

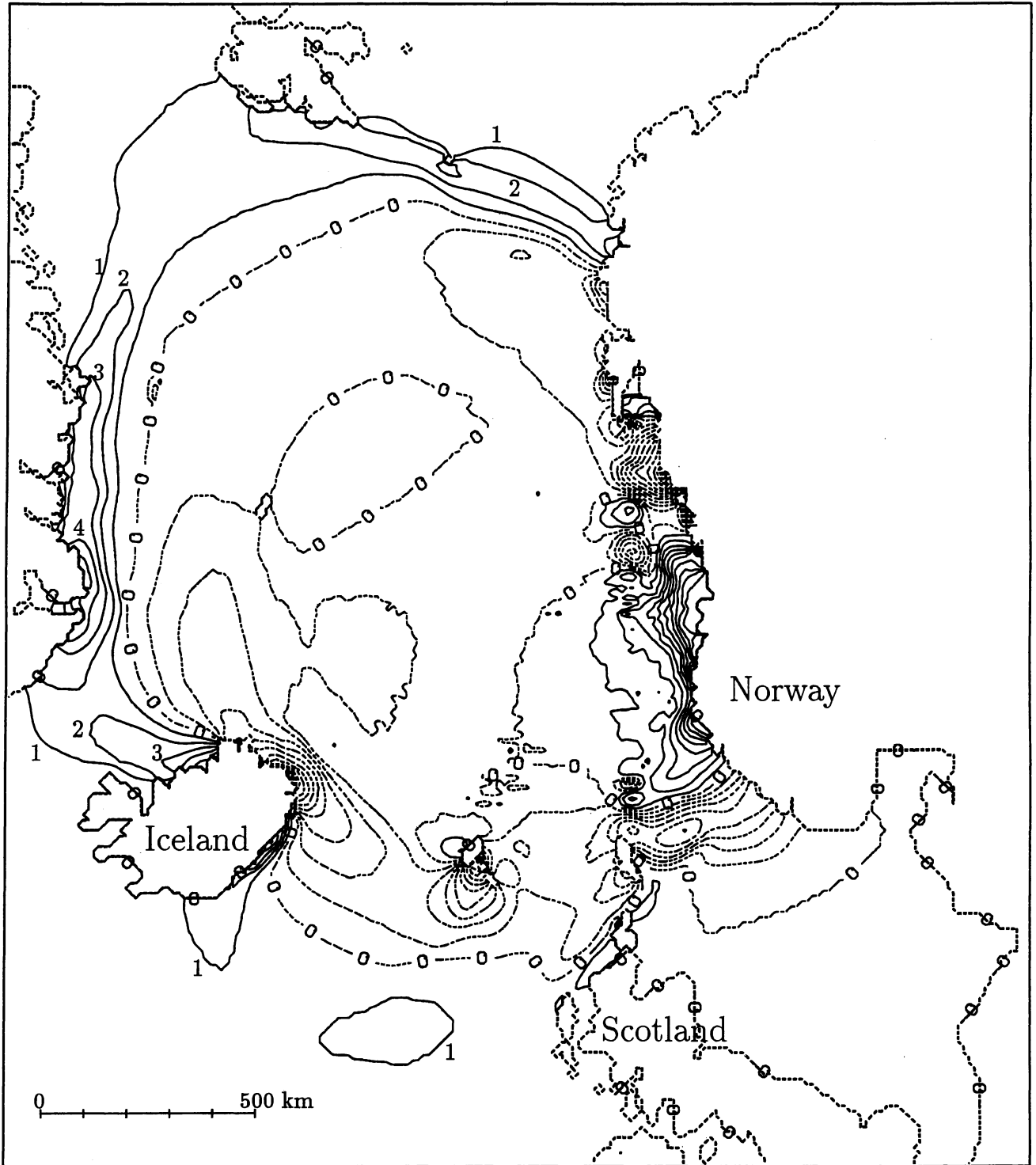t=1 hour

Figure 6:

t=2 hours

Figure 7:

t=2 hours

Figure 8:

t=3 hours

Figure 9: